Atomisation of very viscous liquids

Campanile F.[1], Azzopardi B.J.[1]

1. Multiphase Flow Research Group, School of Chemical Environmental and Mining Engineering, University of Nottingham, University Park, Nottingham NG7 2RD, U.K.

Liquids with viscosities from 5,000 to 50,000 times that of water have been atomised in a twin fluid atomiser. Mechanisms of atomisation together with spray angle, distribution of liquid and drop size distribution have been determined. A model to describe the resulting drop sizes has been developed. This allows for viscous effect and for compressibility in the gas phase.

1. Introduction

Twin-fluid atomisers have been widely used in applications involving viscous fluids as the mechanism of atomisation does not rely on the pressurisation of the liquid phase and the efficient energy transfer. There are two basic types of atomisers: internal mixing or external mixing. Yule and Dunkley [1] refer to the internal mixing as the more suitable configuration to obtain finer sprays for the more efficient mixing between the two phases. Therefore lower gas flow rates are generally used in internal mixing devices. However problems such as blockage and a wider spray angle can lead to the choice of external mixing. The two categories are usually studied separately, mainly for the different geometries involved. However similar correlations are often encountered in the literature, proving that similar mechanisms of atomisation may characterise both systems. More literature available on the external-mixing devices.

Experimental investigations and models of twin-fluid atomisers date back over sixty years [2, 3]. Early studies highlighted the role of the relative velocity between the two liquid and gas phases, and the negative effect of viscosity. Nukiyama and Tanasawa [2] also found that the viscosity effect is negligible if the aerodynamic forces prevail, later confirmed [4, 5] for internal mixing devices.

Effervescent atomisation may well fall in the same category of internal mixing twin fluid atomisers even if they are meant to operate in different conditions. The typical atomisation regime consists in the formation of bubbles capable of breaking the liquid film into drops due to the occurrence of two-phase sonic speed at the nozzle [6]. Increasing the bubble energy is clearly improving atomisation. Whitlow and Lefebvre [7] showed that there is a limit to this behaviour caused by bubble coalescence, which results in the occurrence of annular flow.

Santangelo and Sojka [8] conducted an investigation of the spray structure close to the nozzle for viscosities 0.1-0.8 Pa s and air/liquid mass ratios of 0.01-0.1. For air/liquid mass ratios

<0.02, the spray pattern was characterised by the formation of large bubbles, which then exploded after exiting the nozzle and produced a shower of filaments and a thick ring at the bottom (cap of the bubble). Increasing the gas flow rates leads to a change in the structure with multiple bubbles present at the nozzle exit.

This paper presents an experimental and modelling study of atomisation of liquids with viscosities 5,000 and 50,000 times that of water in a twin fluid atomiser.

2. Experimental arrangements

2.1 Flow facility

The experiments reported here were carried out in the facility shown schematically in Figure 1.a. Liquid is fed from the feed tanks by a positive displacement pump to the mixer through a galvanised steel pipe of 32 mm internal diameter. The liquid flow rate was determined from the fall in the liquid level in the tank. Flow rates between 18 and 100 l/h were employed. Air was supplied by the laboratory mains at a pressure of 540 kPa. The air flow rate was measured by means of an orifice plate connected to a ABB Kent Taylor D.P. cell. Full details are given by Campanile [9].

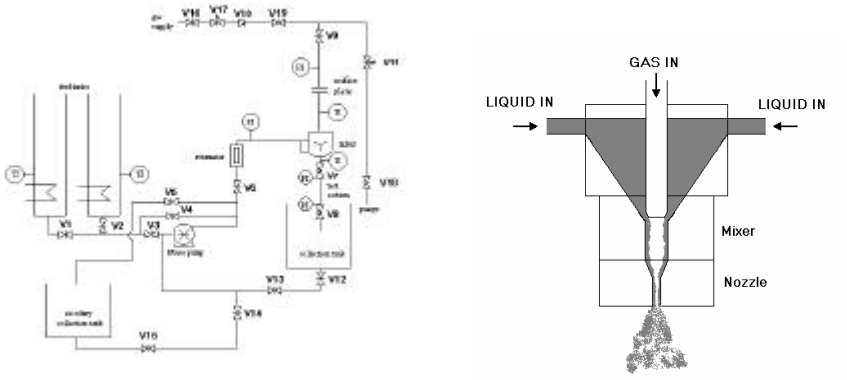

a) b)

Fig. 1 – a) Experimental apparatus, b) Mixer/atomiser.

The mixing unit, shown in Figure 1b, was designed to create annular flow in the nozzle so enhancing interaction between gas and liquid. The gas pipe enters from the top and can be moved up and down over 22 mm to adjust the annular liquid entry. Most of the mixer is made from transparent acrylic resin blocks. Mixing is achieved in the middle section and the flow gradually converges to the 12 mm, 50mm nozzle. The liquid is collected in a cylindrical steel tank.

The liquids employed were tap water and solutions of corn syrup with viscosities of 5 Pa s (95% concentration) and 50 Pa s (100%) which were all essentially Newtonian. As temperature strongly affects the viscosity of the system, the experiments were carried out at 25 ± 2ºC and temperature was monitored in the test section and nozzle. Density was measured with a calibrated measuring glass while surface tension was measured with a de Noüy tensiometer. In calculations the density was taken to be 1250 kg/m^3 and the surface tension 0.08 N/m at 25ºC.

2.2 Spray pattern

A visual investigation was performed in order to determine the mechanisms involved in this process with a HS 4500 Kodak high-speed video camera at a maximum of 4500 frames/sec. The liquid distribution across a representative cross section of the spray was analysed through a purpose built patternator. Measurements were performed collecting the spray into small cylinders. These were held in a tray carrying 21 plastic cylinders, each of 7 cm height and 2.5 cm diameter. The distance from the nozzle was chosen following literature recommendations [10] and experimental evidence from the visual investigation. Once the sampling is completed, each cylinder is weighted and the liquid content calculated. This value is then corrected accounting for the circular cross section of the cylinders and extrapolating it for the case of a square section. Therefore, the final result shows the distribution of the liquid along a rectangular slit of 52.5 cm length and 2.5 cm width. The sampling time was also used to estimate the mass of liquid sprayed over the whole cross-section, scaling the measurements over the entire spray area. All data were within ± 30 % of the corresponding inlet liquid flow rate.

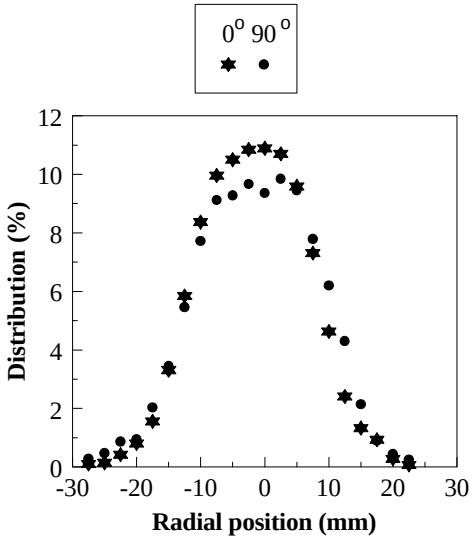

Fig. 2 –Example of comparison for two orthogonal positions along the diameter for a gas superficial velocity of 60 m/s, liquid superficial velocity of 0.15 m/s and a viscosity of 5 Pa s.

The orientation of the patternator was altered to check for spray symmetry. Figure 2 shows one example. All except the lowest gas flow rate runs with water gave similar results. For those conditions an uneven distribution of the liquid flow was observed inside the nozzle, which may be caused by the liquid being dragged by surface tension forces towards one region of the nozzle. This effect is triggered by the microscopic imperfection in the shape of the nozzle and particularly enhanced by low viscosity of water. If the gas flow rate is increased, the height of the peak is not remarkably affected, while the liquid distribution becomes more symmetrical, probably due to the action of the gas flow, which now controls spreading of the liquid over the section.

2.3 Drop size distribution

In the case of water the drop size distribution was measured with a Malvern Particle Analyser 2600 positioned about 500 mm downstream of the end of the nozzle. However, because of

the sizes of the drops produced (> 2 mm), this method was not suitable for the liquids with higher viscosity. A technique based on the collection of drops on a slide was developed for this purpose, a schematic of which is shown in Figure 4. It consists of a hollow cylinder of 80 mm internal diameter and an axial slit of 550 mm long and 15 mm wide located along one side.

The dimensions were chosen from a preliminary analysis of the liquid distribution over the spray cross-section. The width was minimised to limit the disturbance to the flow. A slide covered with a rectangle of black cardboard, chosen for its smoothness and resistance to the liquid and for good photographic contrast, is inserted in the cylinder which was placed perpendicular to the spray axis. The drops deposited on to the slide did not show a significant shape change over two days. Digital photographs and image analysis were then use to determine five parameters for each drop: perimeter, area, major axis, breadth and circularity. Breadth is defined as the longest dimension perpendicular to the major axis. Circularity is the ratio between the perimeter squared and the area (4π for a circle). This technique is restricted to drops diameters > 40 μm due to the resolution of the photo editing software. This limit was well below the typical range of drop size encountered in the experiments, generally characterised by Mass Mean Diameters above 800 μm. The effect of the by-pass of fine droplets was also neglected, as the drops produced are particularly large. Calibrations were carried out by depositing single drops of known size on to the slide. This enabled relationships between the original size and the measured parameters to be developed. Three different types of deposited shapes were considered each with their own relationships: hemispheres, half cylinders and generic irregular spheres.

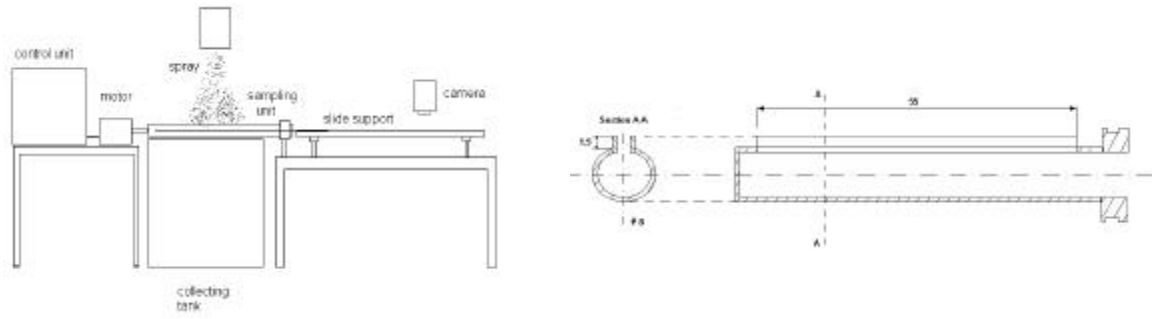

a) b)

Fig. 3 – a) set-up for drop collection and b) sampling device (sizes are in cm).

3. Mechanisms of atomisation

Three different flow regimes were identified in the nozzle for the range of experimental conditions employed at viscosities greater than that of water. They are: slug flow, characterised by the formation of elongated bubbles with size comparable with the tube diameter; froth flow, with thin liquid bridges, which can also occupy the whole cross-section; annular flow, characterised by a thin liquid film flowing in an annulus attached to the wall and the gas flowing in the core. In the case of water, if the gas flow rate is zero, a jet is formed that breaks up according to the Rayleigh mechanism, as also shown by Choi and Lee [11]. There is also evidence of a break-up regime similar to the *purepulsating mode* described by those authors at low gas flow rates. Increasing the gas flow rate, the flow pattern is characterised by the formation of ligaments, similar to the *stretched streamwise*

ligament break-up [12]. A similar mechanism was observed at high viscosity for high gas flow rates, but the wavy pattern is less evident because the higher viscosity, which results in thicker films and smaller amplitude waves. However, it was observed that the ligaments are thicker than in the case of water due to the increase in viscosity. At low flow rates the system shows a peculiar mechanism of atomisation characterised by large bubbles bursting at the nozzle tip. These are formed inside the nozzle and correspond to slug flow. Liquid plugs form periodically and then explode due to the consequent pressure build-up upstream. The result is a shower of small drops that accompanies a thick ring shaped ligament that is deformed but not broken down. Such structures are similar to those reported by Santangelo and Sojka [8]. A peculiar pulsating sound pattern characterises this operating regime. There is also evidence of a transition regime of atomisation in which both of the above mentioned mechanisms above. In other words increasing the gas flow rate, the mechanism characterised by bubbles bursting at the nozzle exit tends to disappear up to the point where a fully developed annular flow occurs. Photographs of the spray patterns taken with at 4500 frames/sec are illustrated in Figure 4.

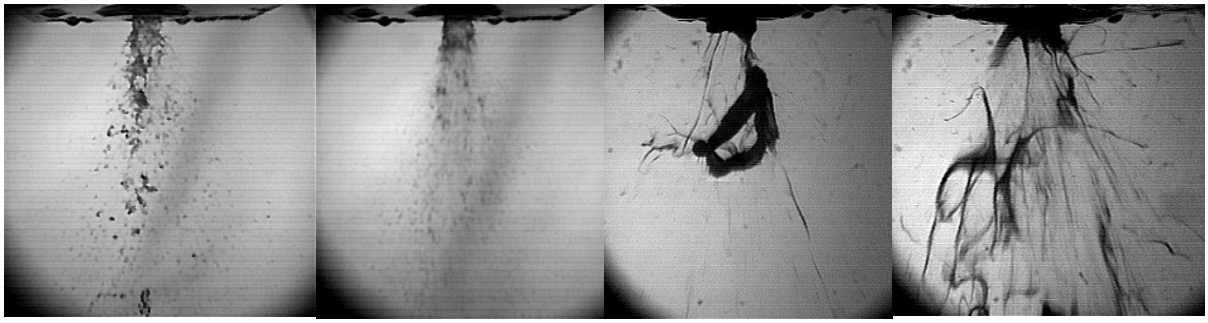

a) b) c) d)

Fig. 4 - Spray pattern close to the nozzle (from the nozzle tip down to 10 diameters distance) for liquid viscosity ≅ 0.001 Pa s and liquid superficial velocity = 0.15 m/s: a) gas superficial velocity = 51 m/s; b) gas superficial velocity = 116 m/s. For liquid viscosity ≅ 5 Pa s and liquid superficial velocity = 0.15 m/s c) gas superficial velocity = 70 m/s; d) gas superficial velocity = 256 m/s. The length of the spray reported is about 10 cm.

A model of atomisation has been developed which follows the original work of Wolfe and Andersen [13], who studied the break-up of a drop in a high-speed gas stream. At high Weber numbers, break-up occurs through a "stripping" mechanism. The drop is deformed showing a convex surface to the flow.

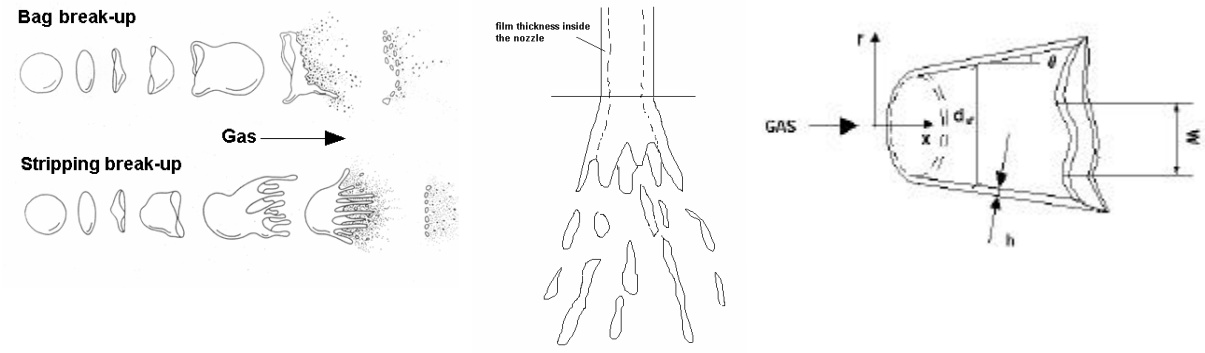

Fig. 5 – a) Mechanisms of break-up of drops; b) schematic representation of the spray in annular regime, c) model of the annular liquid film exiting the nozzle.

Stripping break-up shows characteristics very similar to the atomisation in the present work. Ligaments are formed at the end of the annular film, which then break up producing drops. Wolfe and Andersen [13] assumed the film to break down into "strips" of liquid of width, W, due to the effect of the film divergence, which thins the film. Each strip behaves as a thin flat film, whose break-up into drops is assumed to be controlled by the growth of instabilities on the surface according to the mechanism described by Dombrowski and Hooper [14]. The mean drop diameter was obtained from the resulting element of liquid from:

$$D = \sqrt[3]{\frac{6W\lambda_{opt}h}{\pi}} \tag{1}$$

Where λ_{opt} is the wavelength of that disturbance.

Observation from high-speed videos shows that the ligaments created from the liquid film are produced by the effect of the gas on the liquid surface. This differs from the mechanism suggested by Wolfe and Andersen [13]. The ligaments are formed from the interaction between the gas shear force and gravity, which tend to pull the ligament from the annular film rim, and the surface tension, which acts against the formation of new liquid surface. This case is similar to that analysed by Azzopardi [15] investigating the behaviour of liquid film at the edge of a plate interacting with a gas stream. He adapted ideas of G.I. Taylor to produce a model for instability of an interface subject to a perpendicular acceleration. The optimum wavelength for this lateral instability which will give us W is given by

$$\lambda_{w\,opt} = 2\pi\sqrt{\frac{3\sigma}{\rho_l A_c}} \quad \text{where} \quad A_c = \frac{1}{\rho_l}\frac{dp}{dx} + g \tag{2}$$

Here equations were provided for the pressure gradient based on equations appropriate to the viscosities studied. Longitudinal break up was calculated from the inviscid [16] and viscous [17] models. For the former the half the wavelength of the fastest growing instability is given by:

$$\lambda_{opt} = \frac{4\pi\sigma}{\rho_g U_r^2} \tag{3}$$

4. Results and discussion

The variation in spray angle is seen to be much smaller at velocities greater than 50 m/s than below. There is little effect of viscosity, Figure 6. The patternator results show that the liquid is very tightly grouped at low gas velocities and spreads out as the gas velocity increases, Figure 7. Examples of the distribution of drop sizes are show in Figure 8. Figure 8a shows the higher viscosity data (50 Pa s) at a liquid superficial velocity of 0.15 m/s whilst Figure 8b shows measurements from the 5 Pa s at a liquid superficial velocity of 0.07 m/s. It can be seen that there are bimodal distribution at lower gas velocities. However, the distributions are single peaked at the high gas velocities.

The model described above was found to give reasonable predictions of the water data. Versions of the model were produced using different assumptions – viscous/inviscid and incompressible/compressible. For compressibility, the approach of Ibrahim [18] was adapted. There was little variation between the variants of the model for water. However, Figure 9 shows that the viscous model performs much better for the very viscous liquids particularly at

higher air velocities. It is suggested that the poor agreement at lower gas velocities might be related to the presence of two peaks in the drop size distributions illustrated in Figure 8.

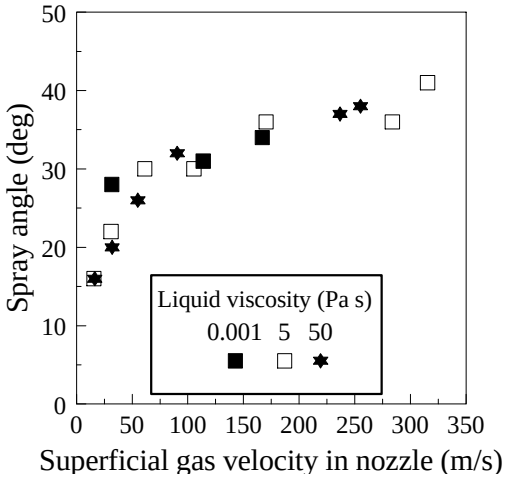

Fig. 6 - Effect of gas velocity and liquid viscosity on spray angle

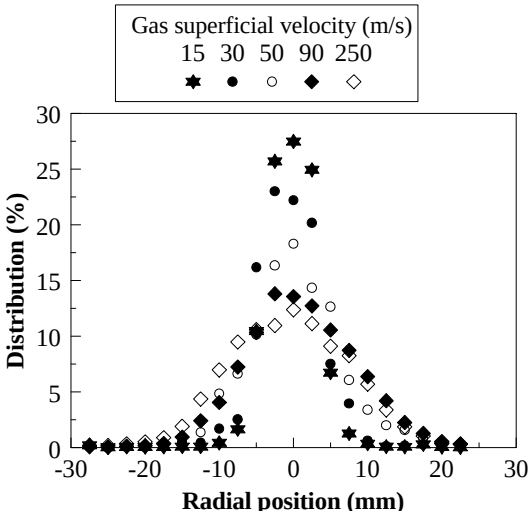

Fig. 7 – Distribution of liquid as measured by the patternator. Liquid superficial velocity = 0.15 m/s, liquid viscosity = 50 Pa s.

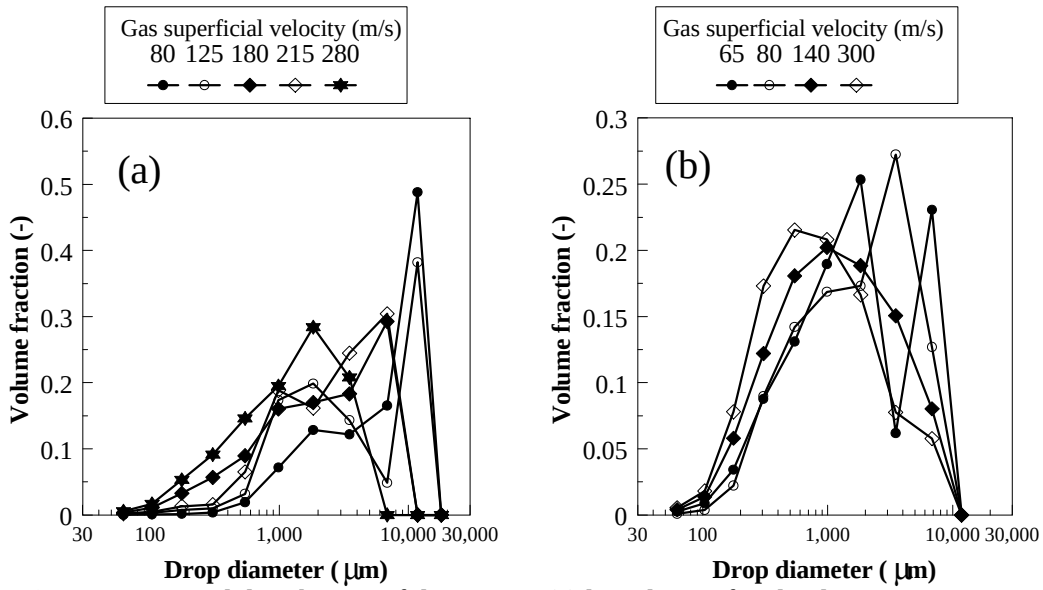

Fig. 8 – Measured distribution of drop sizes. (a) liquid superficial velocity = 0.15 m/s, viscosity = 50 Pa s; (b) liquid superficial velocity = 0.07 m/s, viscosity = 5 Pa s.

Predictions from the models have been compared with data from an effervescent atomiser [8] and good agreement has been obtained. From this it is suggested that the "tree" structure described in their observation probably corresponds to an annular film, which breaks down into drops be the mechanism postulated above.

The effect of the bimodal distributions at lower gas velocities has been modelled by use of two Rosin-Rammler distributions. This indicates that the fraction in one of the distributions varies systematically from 0 to 1.

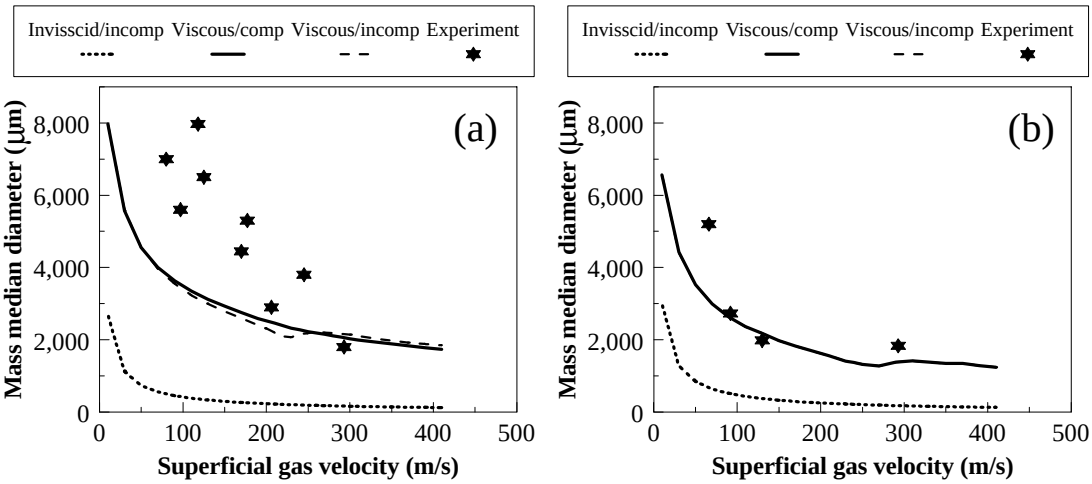

Fig 9 – Comparison between experimental data and proposed models: (a) liquid viscosity = 50 Pa s, liquid superficial velocity = 0.15 m/s; (b) liquid viscosity = 5 Pa s liquid superficial velocity = 0.07 m/s.

5. Conclusions

1. The efficacy of creation of small drops depends on the flow pattern occurring in the nozzle.
2. The drop size distribution is bimodal at lower gas velocities and has a single peak when the velocity is high.
3. A model which considers the circumferential and axial break up of the liquid film can give good predictions of drop size if compressibility and viscous effects are considered

6. Acknowledgements

The authors would like to thank ICI for sponsoring this work.

7. References

[1] Yule A J and Dunkley J J 1994 *Atomisation of Melts for Power Production and Spray Deposition* (Oxford, Clarendon Press).
[2] Nukiyama S and Tanasawa Y 1939 *Trans. Soc. Mech. Eng. Japan* **5** 68-75.
[3] Wigg L D 1964 *J. Inst. Fuel* **37** 500-505.
[4] Lefebvre A H 1980 *Prog. Energy Combust. Sci.* **6** 233-261.
[5] Rizk N K and Lefebvre A H 1984 *J. Eng. Gas Turbine* **106**. 634-638.
[6] Chawla J M 1985 *Proc. ICLASS-85*, London Paper LP/1A/5/1-7.
[7] Whitlow P B and Lefebvre A H 1993 *Atomization and Sprays* **3** 137-155.
[8] Santangelo P J and Sojka P E 1995 *Atomization and Sprays* **5** 137-155.
[9] Campanile F 2000 PhD Thesis, University of Nottingham.
[10] Lasheras J C, Villermaux E, and Hopfinger E J 1998 *J. Fluid Mech.* **357** 351-379.
[11] Choi C J and Lee S Y 1997 *Proc. ICLASS-97*, Seoul, August 18-22, 225-261.
[12] Stapper B E, Sowa W A and Samuelsen G S 1992 *J. Eng. Gas Turb. Power* **114** 39-45.
[13] Wolfe H E and Andersen W H 1965 *Proc. Int. Shock Tube Symposium*, Naval Ordinance Lab, White Oak, Maryland, USA, 1145-1152.
[14] Dombrowski N and Hooper P C 1962 *Chem. Engng. Sci* **17** 291-305.
[15] Azzopardi B J 1994 *Nucl. Eng. Design* **154** 257-262.
[16] Squire H B 1953 *J. App. Phys.* **4** 167-169.
[17] Senecal P K, Schmidt D P, Nouar I, Rutland C J, Reitz R D, and Corradini M L 1999 *Int. J. Multiphase Flow* **25** 1073-1097.
[18] Ibrahim E A 1997 *Chem. Eng. Comm.* **161** 25-44.